Electronic Supplementary Material (ESI) for Materials Advances.
This journal is © The Royal Society of Chemistry 2022

Electronic Supplementary Information (ESI)

Pore-confined cobalt sulphide nanoparticles in a metal–organic framework as a catalyst for colorimetric detection of hydrogen peroxide

You-Liang Chen,[a] Yi-Ching Wang,[a] Yu-Hsiu Chen,[a] Tzu-En Chang,[a] Cheng-Hui Shen,[a] Chi-Wei Huang [a] and Chung-Wei Kung [*a]

[a] Department of Chemical Engineering, National Cheng Kung University, Tainan City, Taiwan, 70101.

*Email: cwkung@mail.ncku.edu.tw

S1. Additional data for materials characterization

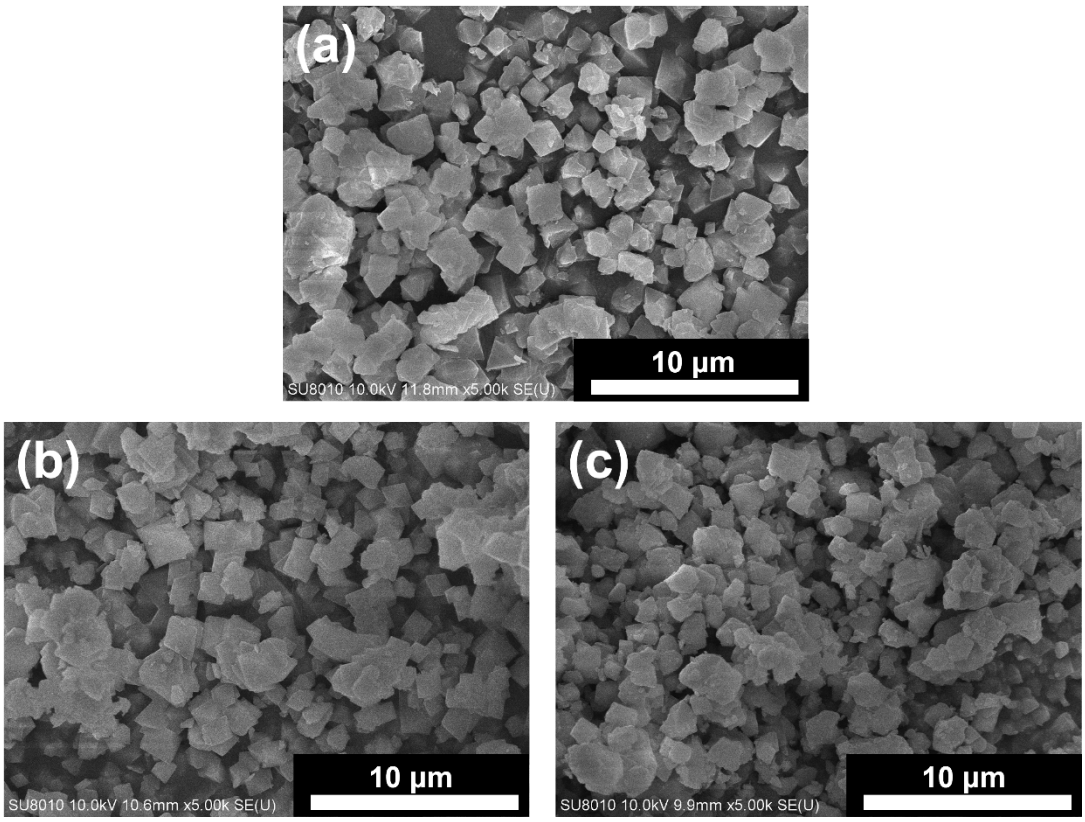

Figure S1. SEM images of (a) MOF-808, (b) Co-MOF-808, and (c) CoS-MOF-808.

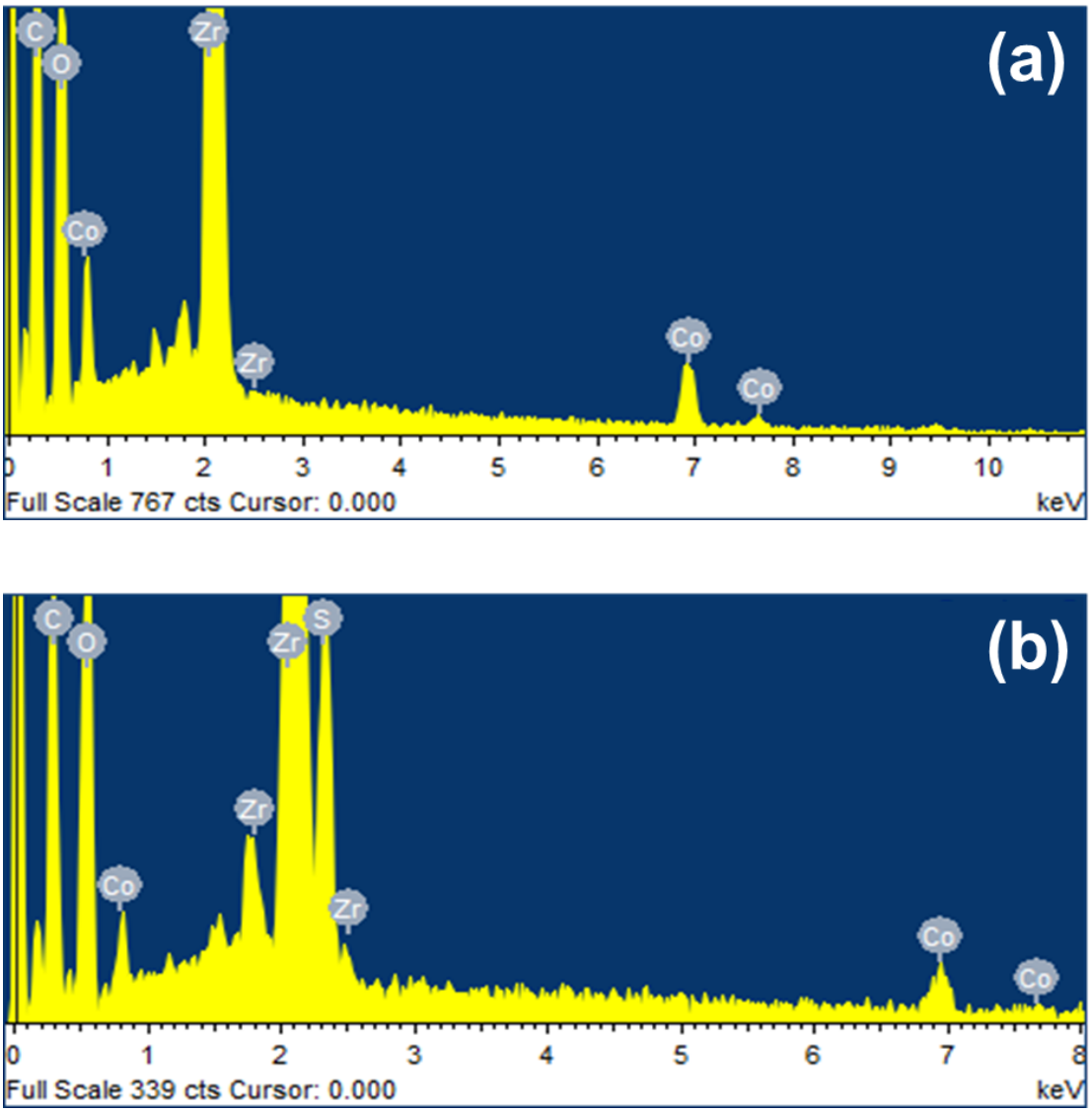

Figure S2. Representative EDS spectra of (a) Co-MOF-808, and (b) CoS-MOF-808.

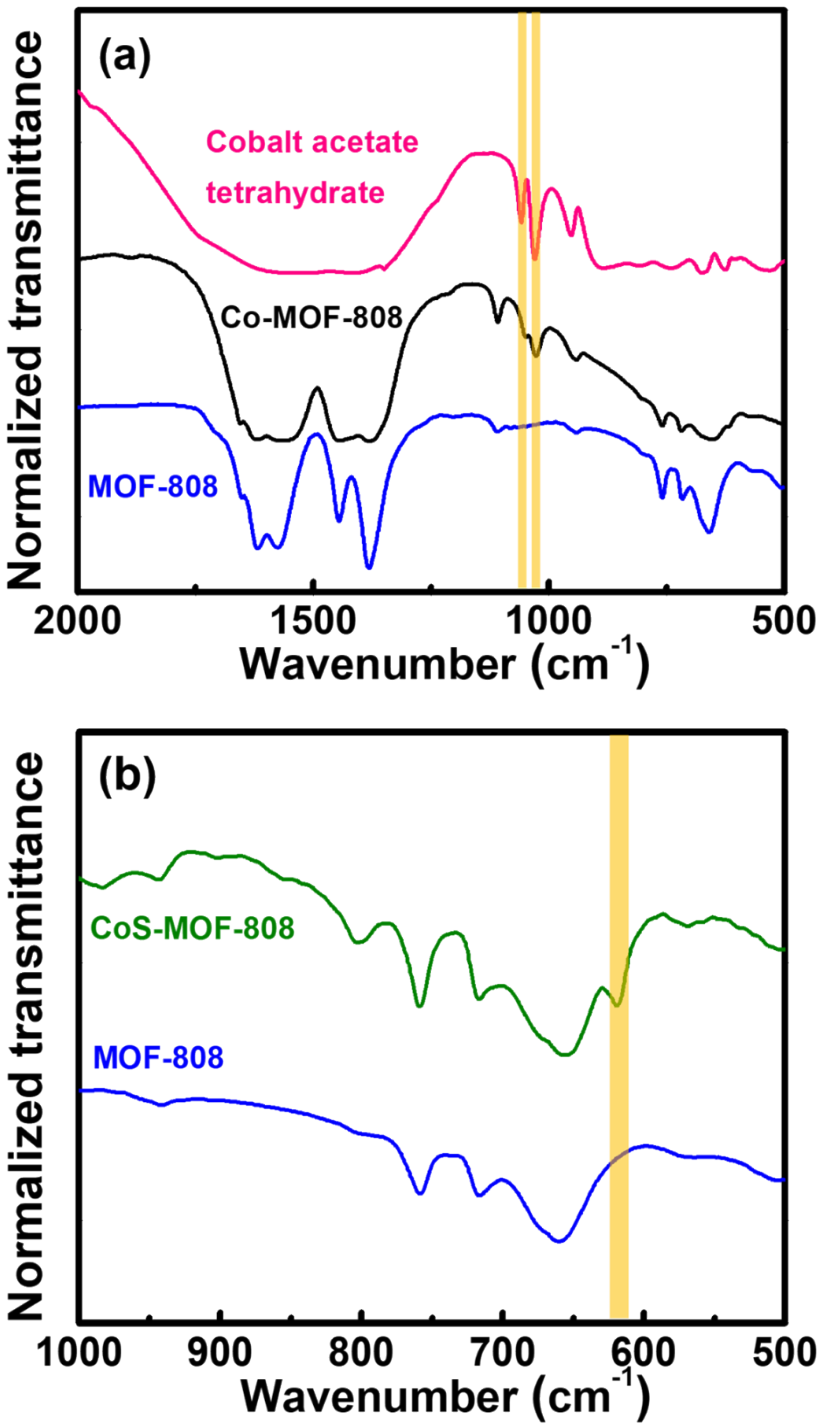

Figure S3. FTIR spectra of (a) MOF-808, Co-MOF-808 and cobalt acetate tetrahydrate, and (b) MOF-808 and CoS-MOF-808. Characteristic peaks of acetate ions and cobalt sulphide are highlighted in orange in (a) and (b), respectively.

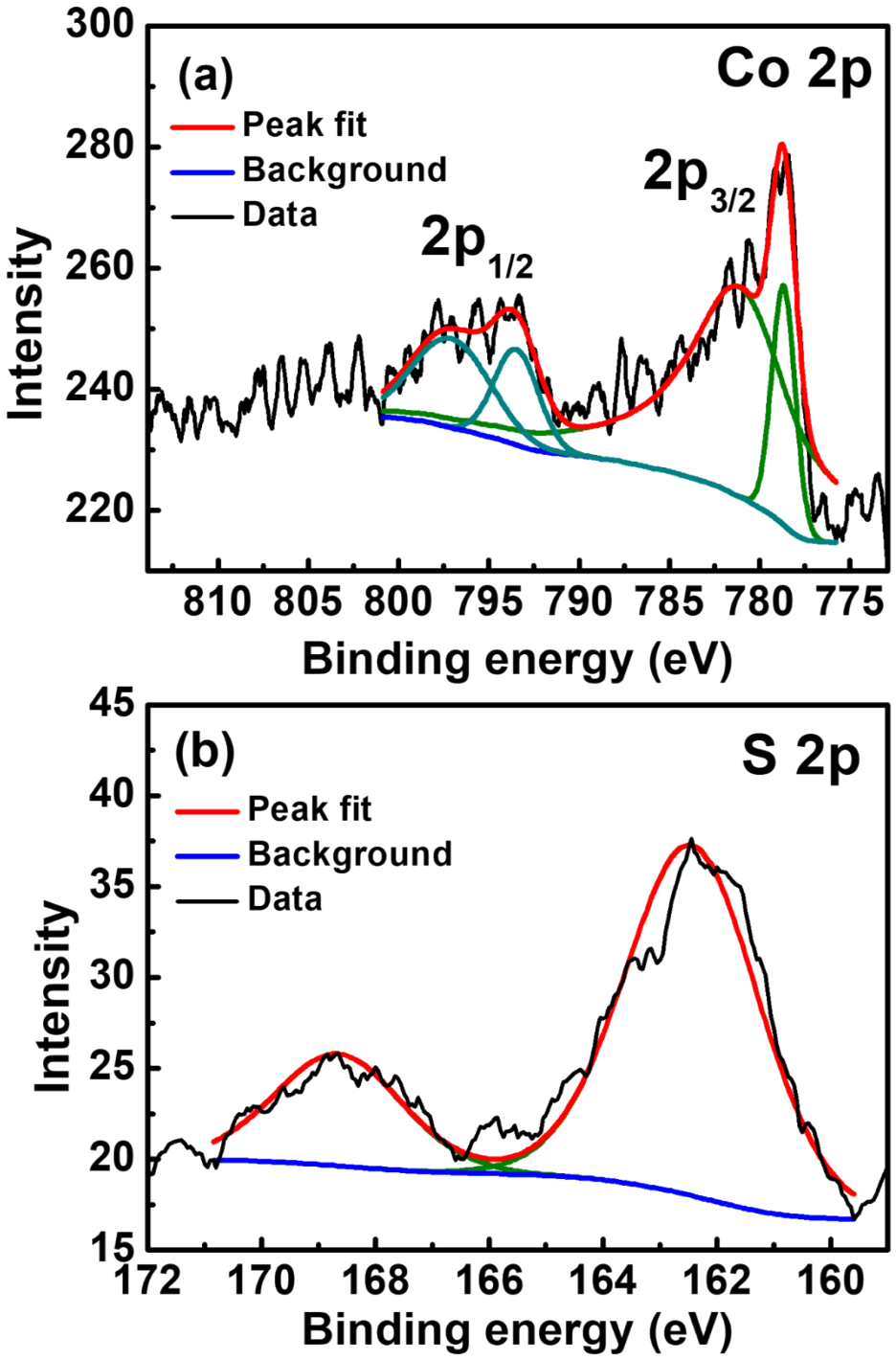

Figure S4. XPS spectra of CoS-MOF-808 in the regions of (a) Co 2p and (b) S 2p.

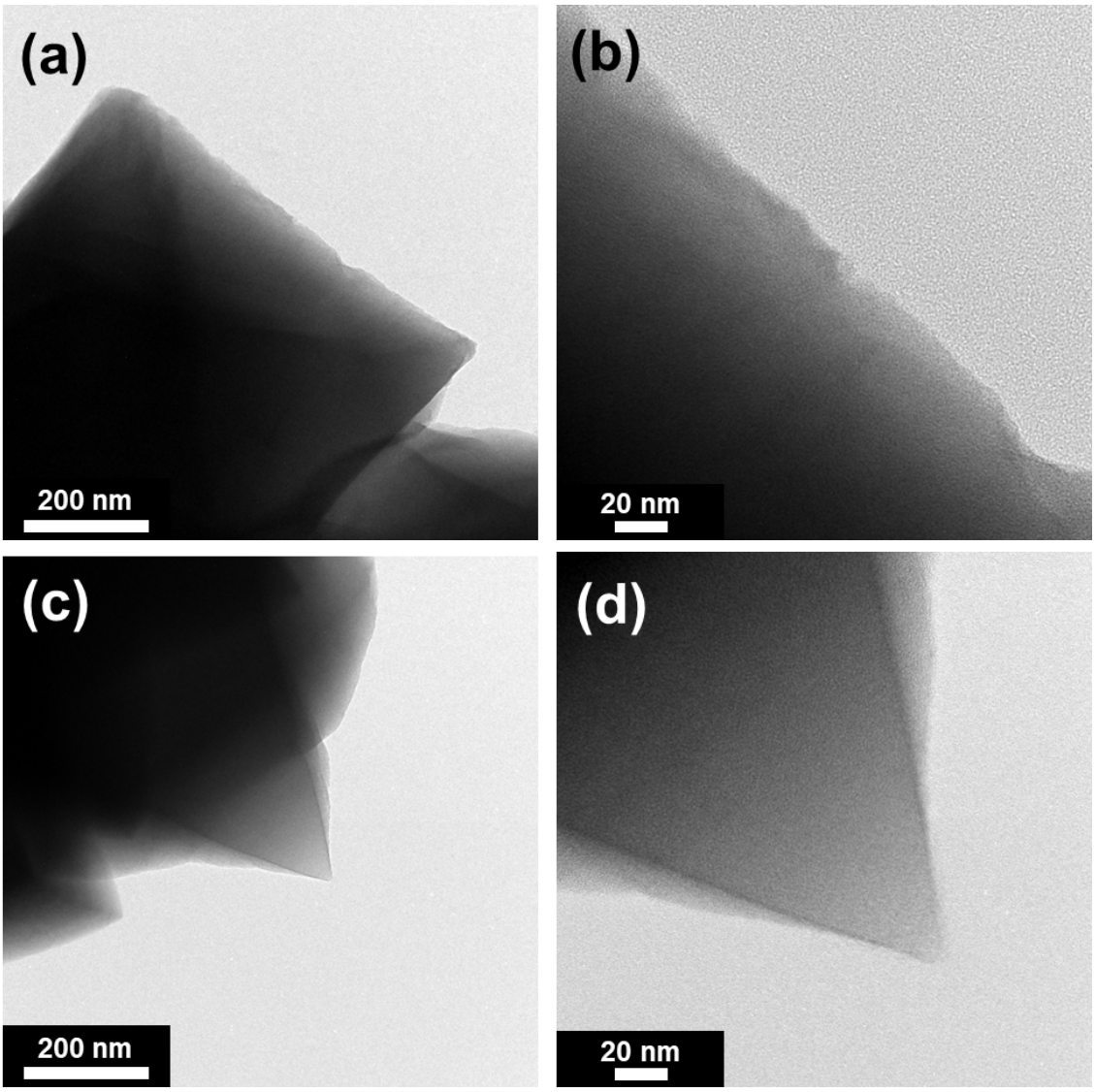

Figure S5. Representative TEM images of (a-b) MOF-808, and (c-d) Co-MOF-808.

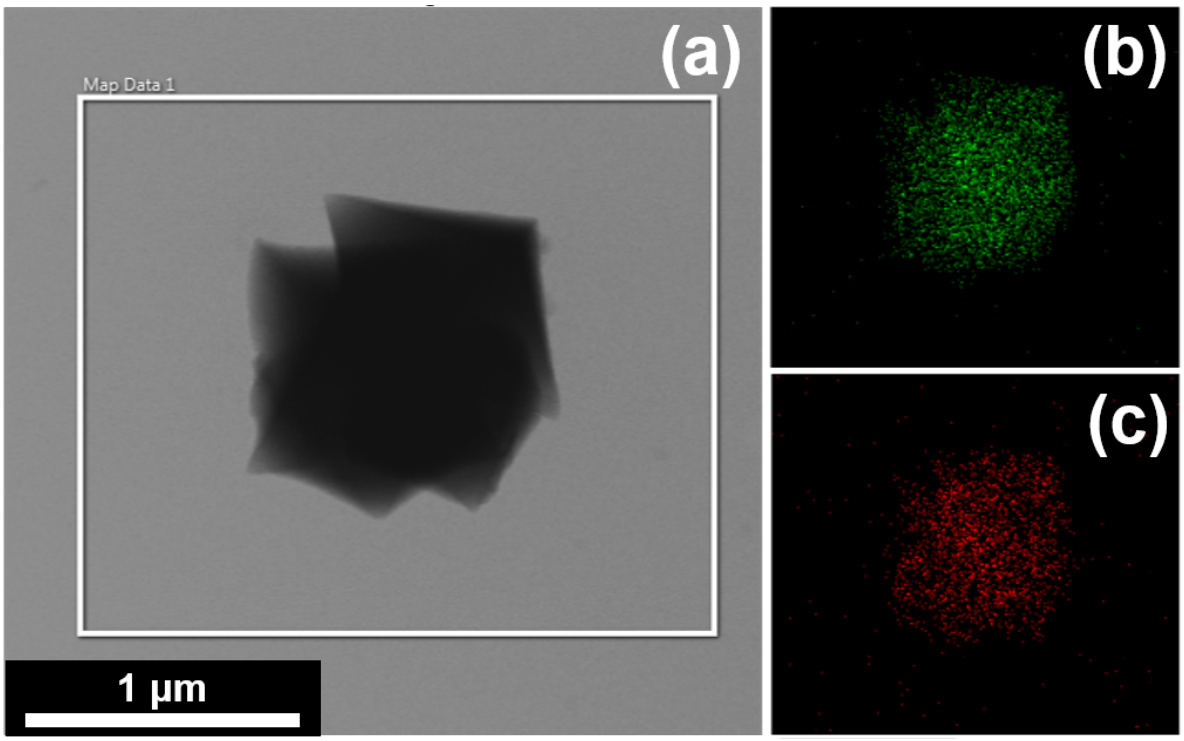

Figure S6. (a) TEM image of Co-MOF-808. Corresponding EDS elemental mapping signals of (b) zirconium, and (c) cobalt, collected from the rectangular region indicated in (a).

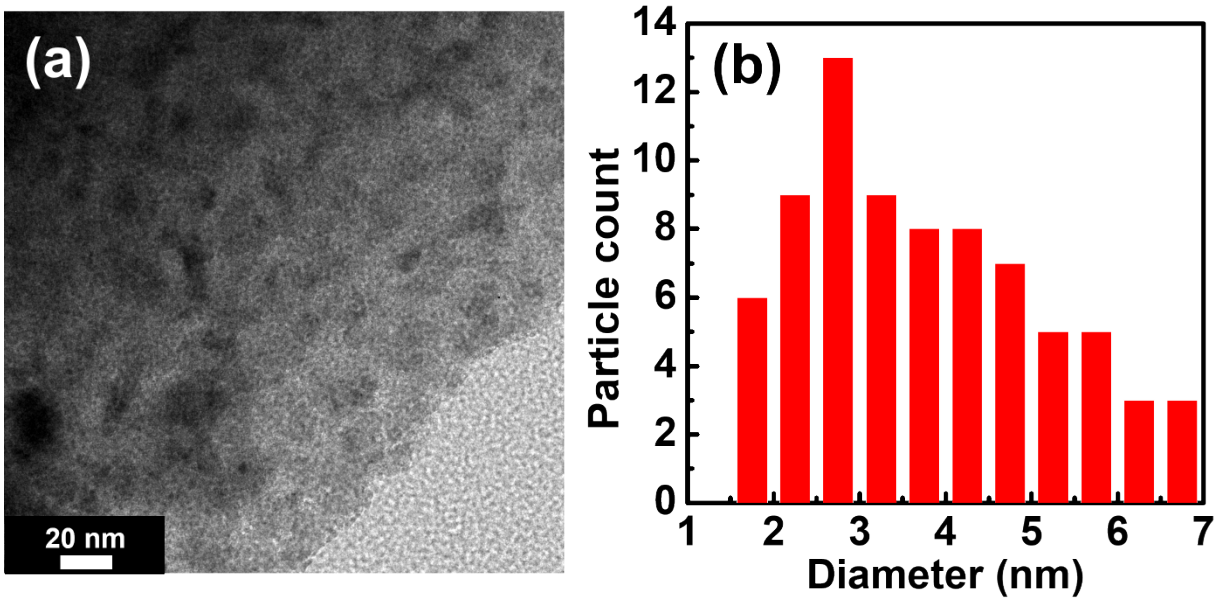

Figure S7. (a) TEM image of CoS-MOF-808. (b) Particle size distribution of cobalt sulphide nanoparticles present in CoS-MOF-808 estimated from (a).

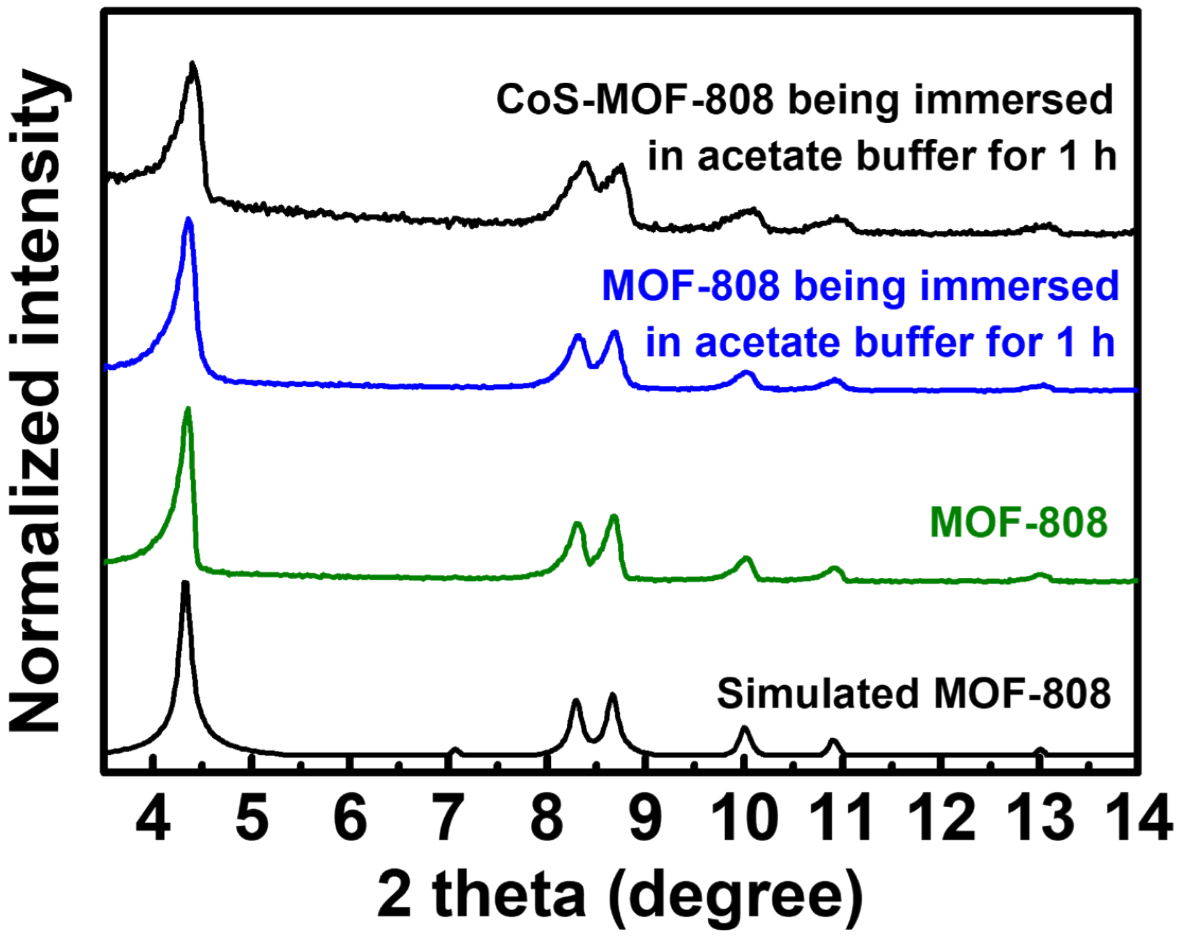

Figure S8. PXRD patterns of the CoS-MOF-808 and pristine MOF-808, which were immersed in the acetate buffer solutions (0.1 M, pH = 4.03) for 1 h followed by the successive washing steps with water and solvent exchange with acetone for three times over the course of 24 h, sequentially.

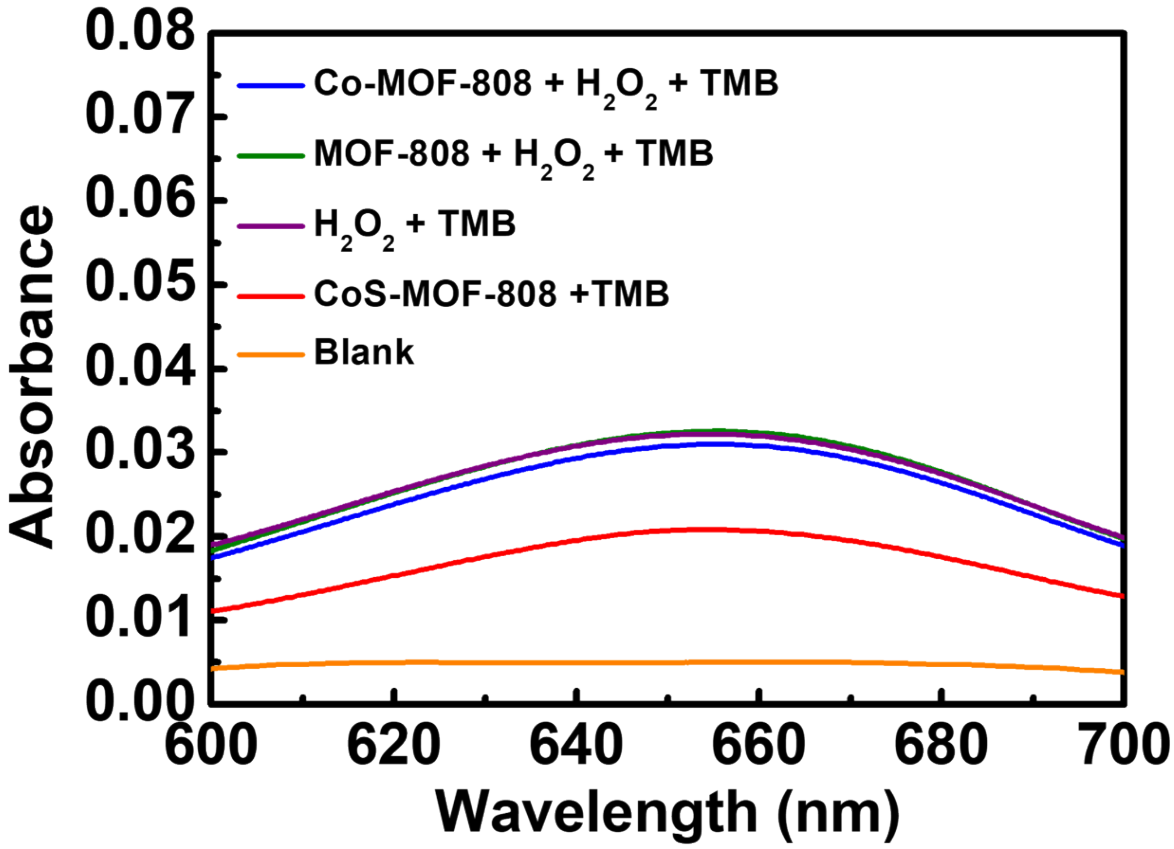

Figure S9. Magnified version of the UV-vis spectra shown in Figure 4 of the main text.

S2. Determination of TON

Mole of oxTMB generated owing to the presence of CoS-MOF-808 in the 200-mL solution:

$$N_{oxTMB} = \frac{1.024 - 0.057}{39000} \times \frac{200}{1000} = 4.96 \times 10^{-6}\ (mol)$$

From ICP-OES data, the loading of cobalt in CoS-MOF-808 is 1.32 Co per node, and as suggested by the ICP-MS result, the chemical composition of these pore-confined nanoparticles is $CoS_{1.69}$. By utilizing the molecular weight of MOF-808 containing one hexa-zirconium node (*i.e.*, 1,363 g/mol), the molecular weight (MW) of CoS-MOF-808 can be calculated:

$$MW = 1363 + 1.32 \times 59 + 1.32 \times 1.69 \times 32 = 1512\ (g/mol)$$

Mole of all cobalt atoms present in 2 mg of the catalyst added in the 200-mL solution:

$$N_{Co} = \frac{2 \times 10^{-3}}{1512} \times 1.32 = 1.75 \times 10^{-6}\ (mol)$$

$$TON = \frac{N_{oxTMB}}{N_{Co}} = 2.83$$

S3. Kinetic experiments

Experimental details for kinetic experiments can be found in the Experimental Section of the main text. With H_2O_2 as the substrate and a fixed concentration of TMB at 0.5 mM, the absorbance of samples at 652 nm (A) after terminating the reaction at various reaction times (t) were measured in order to obtain dA/dt at each concentration of H_2O_2 (Table S1). Thereafter, based on the extinction coefficient of oxTMB at 652 nm, *i.e.*, 39000 M^{-1} cm^{-1}, Lambert-Beer's law was used to estimate the initial reaction rate (V_0) at each concentration of H_2O_2, as listed in Table S1. The similar set of experiments were also conducted by serving TMB as the substrate and fixing the concentration of H_2O_2 at 35 mM, and the results are summarized in Table S2. Lineweaver-Burk plots were thereafter constructed for both sets of data, and the results are shown in Figure S10(a) and Figure S10(b). The slope and intercept shown in each Lineweaver-Burk plot represent K_m/V_{max} and $1/V_{max}$, respectively. The K_m and V_{max} for each substrate can then be calculated from the slope and intercept of the corresponding Lineweaver-Burk plot.

Table S1. Values of dA/dt and V_0 for H_2O_2 with CoS-MOF-808 as the catalyst, in the presence of 0.5 mM of TMB.

H_2O_2 concentration (mM)	dA/dt (s^{-1})	V_0 ($M\ s^{-1}$)
25	0.00691	1.77×10^{-7}
30	0.00761	1.95×10^{-7}
35	0.00827	2.12×10^{-7}
40	0.00892	2.29×10^{-7}
45	0.00928	2.38×10^{-7}

Table S2. Values of dA/dt and V_0 for TMB with CoS-MOF-808 as the catalyst, in the presence of 35 mM of H_2O_2.

TMB concentration (mM)	dA/dt (s^{-1})	V_0 ($M\ s^{-1}$)
0.4	0.00897	2.30×10^{-7}
0.45	0.00945	2.42×10^{-7}
0.5	0.0100	2.56×10^{-7}
0.55	0.0101	2.59×10^{-7}
0.6	0.0102	2.62×10^{-7}

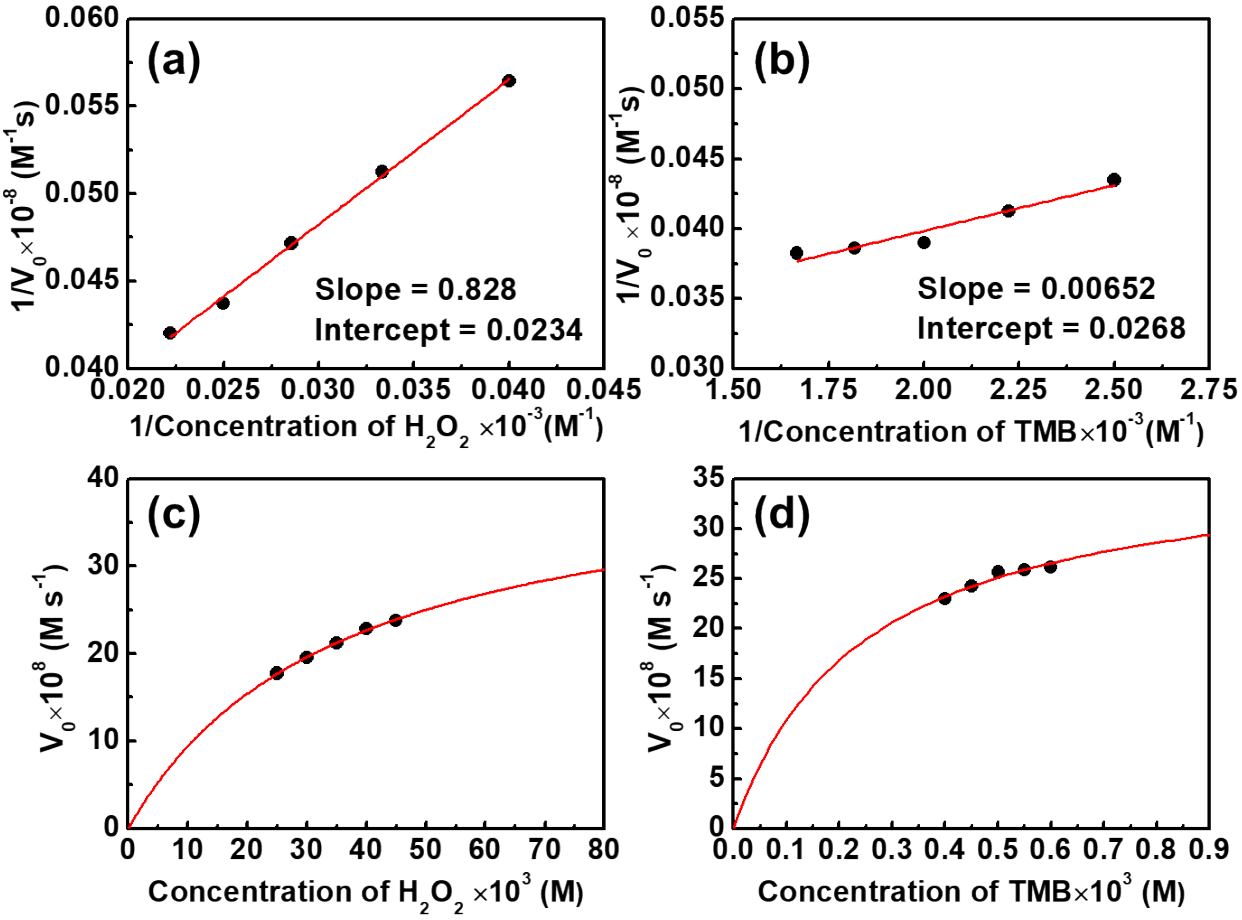

Figure S10. Lineweaver-Burk plots for the CoS-MOF-808 catalyst, obtained by serving (a) H_2O_2 as the substrate in the presence of 0.5 mM of TMB and (b) TMB as the substrate in the presence of 35 mM of H_2O_2. (c-d) Michaelis–Menten models constructed from the data present in (a) and (b), respectively.

Table S3. Partial list of the kinetic parameters of different active materials reported for H_2O_2/TMB reaction and the comparison to those of CoS-MOF-808.

Active material	Substrate	Parameter		Reference
		K_m [mM]	V_{max} [10^{-8} M s^{-1}]	
Fe_3O_4 NPs [a]	TMB	0.098	3.44	[1]
	H_2O_2	154	9.78	
RuO_2 NPs [a]	TMB	0.236	-	[2]
	H_2O_2	212	-	
CoS	TMB	0.41	5.82	[3]
	H_2O_2	7.15	2.65	
WS_2	TMB	1.83	4.31	[4]
	H_2O_2	0.24	4.52	
Co_3S_4 NSs [b]	TMB	0.15	33	[5]
	H_2O_2	58.3	33	
PCN-222 (Fe)	TMB	1.63	-	[6]
	H_2O_2	-	-	
MIL-88 (Fe)	TMB	0.83	6.32	[7]
	H_2O_2	0.12	4.30	
Hemin@ZIF-8	TMB	0.024	0.91	[8]
	H_2O_2	65.08	4.2	
MOF (Co/2Fe)	TMB	0.25	3.78	[9]
	H_2O_2	4.22	4.91	
Au@NH_2-MIL-125 (Ti)	TMB	0.2	-	[10]
	H_2O_2	1.75	-	
CoS-MOF-808	TMB	0.24	37.31	This work
	H_2O_2	35.39	42.73	

[a] NPs = Nanoparticles
[b] NSs = Nanosheets

Table S4. Partial list of the reported colorimetric H_2O_2 sensors and the comparison between their performances and that of the CoS-MOF-808-based sensor.

Active material	Performance		Reference
	LOD (μM)	Linear range (μM)	
Fe_3O_4 NPs [a]	3	5-100	[11]
VO_2 NBs [b]	0.28	1-400	[12]
50Co/CuS-MMT [c]	2.2	10-100	[13]
CuS NRs [d]	0.11	1-1000	[14]
MoS_2/PPY [e]	45	50-2000	[15]
CoS	20	50-800	[3]
MIL-68	0.256	3-40	[16]
MIL-53(Fe)	0.13	0.95-480	[17]
ZIF-67/rGO [f]	3.81	7.5-750	[18]
Cu-MOF	0.42	1-1000	[19]
MOF (Co/2Fe)	5	10-100	[9]
FePt@MIL-101	18.9	40-800	[20]
PB [g] @MIL-101	0.15	2.4-100	[21]
CoS-MOF-808	7.51	50-600	This work

[a] NPs = Nanoparticles
[b] NBs = Nanobelts
[c] MMT = Montmorillonite
[d] NRs = Nanorods
[e] PPY = Polypyrrole
[f] rGO = Reduced graphene oxide
[g] PB = Prussian blue

References:

1. L. Gao, J. Zhuang, L. Nie, J. Zhang, Y. Zhang, N. Gu, T. Wang, J. Feng, D. Yang, S. Perrett and X. Yan, *Nat. Nanotechnol.*, 2007, **2**, 577-583.
2. H. Deng, W. Shen, Y. Peng, X. Chen, G. Yi and Z. Gao, *Chem. Eur. J.*, 2012, **18**, 8906-8911.
3. H. Yang, J. Zha, P. Zhang, Y. Xiong, L. Su and F. Ye, *RSC Adv.*, 2016, **6**, 66963-66970.
4. T. Lin, L. Zhong, Z. Song, L. Guo, H. Wu, Q. Guo, Y. Chen, F. Fu and G. Chen, *Biosens. Bioelectron.*, 2014, **62**, 302-307.
5. S. Hashmi, M. Singh, P. Weerathunge, E. L. H. Mayes, P. D. Mariathomas, S. N. Prasad, R. Ramanathan and V. Bansal, *ACS Appl. Nano Mater.*, 2021, **4**, 13352-13362.
6. D. Feng, Z. Y. Gu, J. R. Li, H. L. Jiang, Z. Wei and H. C. Zhou, *Angew. Chem. Int. Ed.*, 2012, **51**, 10307-10310.
7. C. Gao, H. Zhu, J. Chen and H. Qiu, *Chin. Chem. Lett.*, 2017, **28**, 1006-1012.
8. D. Li, S. Wu, F. Wang, S. Jia, Y. Liu, X. Han, L. Zhang, S. Zhang and Y. Wu, *Mater. Lett.*, 2016, **178**, 48-51.
9. H. Yang, R. Yang, P. Zhang, Y. Qin, T. Chen and F. Ye, *Microchim. Acta*, 2017, **184**, 4629-4635.
10. Y. Zhang, J. Song, Q. Pan, X. Zhang, W. Shao, X. Zhang, C. Quan and J. Li, *J. Mater. Chem. B*, 2020, **8**, 114-124.
11. H. Wei and E. Wang, *Anal. Chem.*, 2008, **80**, 2250-2254.
12. G. Nie, L. Zhang, J. Lei, L. Yang, Z. Zhang, X. Lu and C. Wang, *J. Mater. Chem. A*, 2014, **2**, 2910-2914.

13. K. Wu, W. Li, S. Zhao, W. Chen, X. Zhu, G. Cui, Z. Liu, Q. Liu, X. Zhang and X. Zhang, *Colloids Surf. A: Physicochem. Eng. Asp.*, 2020, **602**, 125063.

14. J. Guan, J. Peng and X. Jin, *Anal. Methods*, 2015, **7**, 5454-5461.

15. M. Chi, Y. Zhu, L. Jing, C. Wang and X. Lu, *Anal. Chim. Acta*, 2018, **1035**, 146-153.

16. J. W. Zhang, H. T. Zhang, Z. Y. Du, X. Wang, S. H. Yu and H. L. Jiang, *Chem. Commun.*, 2014, **50**, 1092-1094.

17. L. Ai, L. Li, C. Zhang, J. Fu and J. Jiang, *Chem. Eur. J.*, 2013, **19**, 15105-15108.

18. D. Lu, J. Li, Z. Wu, L. Yuan, W. Fang, P. Zou, L. Ma and X. Wang, *J. Colloid Interface Sci.*, 2022, **608**, 3069-3078.

19. F. Liu, J. He, M. Zeng, J. Hao, Q. Guo, Y. Song and L. Wang, *J. Nanopart. Res.*, 2016, **18**, 106.

20. Z. Hu, Y. Yin, Q. Liu and X. Zheng, *Analyst*, 2019, **144**, 2716-2724.

21. F. Cui, Q. Deng and L. Sun, *RSC Adv.*, 2015, **5**, 98215-98221.